Article

“Burning Lamp”-like Robust Molecular Enrichment for Ultrasensitive Plasmonic Nanosensors

Rui Hao, Hongjun You, Jie Zhu, Teng Chen, and Jixiang Fang

ACS Sens., **Just Accepted Manuscript** • DOI: 10.1021/acssensors.9b02423 • Publication Date (Web): 10 Feb 2020

“Burning Lamp”-like Robust Molecular Enrichment for Ultrasensitive Plasmonic Nanosensors

Rui Hao,[†] Hongjun You,[‡,*] Jie Zhu,[§] Teng Chen,[§,*] and Jixiang Fang[†,*]

[†]Key Laboratory of Physical Electronics and Devices of Ministry of Education, School of Electronic Science and Engineering, Xi’an Jiaotong University, Xi’an, 710049, China

[‡]School of Science, Xi’an Jiaotong University, Xi’an, 710049, China

[§]College of Forensic Medicine, Xi’an Jiaotong University Health Science Center, Xi’an, 710061, China

ABSTRACT: Enriching and locating target analytes into specific "hot spot" are vital for ultrasensitive molecular identification and detection using plasmonic-based techniques. Inspired by mass transportation in lamp wicks, we develop an effective enrichment strategy for highly diluted analytes, in which analytes and Au nanoparticles are transported via solution microflow under the capillarity driving force of glass fiber papers to a heated region. After evaporation, a large volume of solution contained analytes and Au nanoparticles are condensed into a very limited area, and thus, analyte molecules are effectively enriched and located into SERS hot spots. Using this enrichment strategy, the sensitivity and detection limits of SERS are remarkably improved. Detection levels of crystal violet and anthracene are down to 10^{-16} M and 10^{-10} M, respectively. This enrichment strategy is very robust and easy to implement, and it can potentially be exploited in various plasmonic-based molecular detection and identification techniques.

KEYWORDS: surface enhanced Raman scattering, enrichment, capillary force, heating evaporation, ultrasensitive detection

Molecular identification and detection based on plasmonic techniques provide an unprecedented opportunity for investigations in fields such as analytical chemistry, life science, and biomedicine.[1-4] Detecting analytes with ultrasensitivity in highly dilute solutions is fundamentally important and remains a great challenge. Plasmonic coupling effect, which is excited by collective oscillations of free electrons in a nanotextured noble-metal surface, generates "hot spot" for the enhanced Raman scatting.[5,6] In last decades, extensive studies have focused on structural optimization with different types of hot spots, such as nanogaps, nanotips, and nanopores, to investigate interactions between light and nanostructures and to improve detection sensitivity.[7-9] Extraordinary success in single-molecule investigations has been achieved in laboratory with well-constructed nanostructures that concentrate optical radiation energy in hot spots.[10-12] Unfortunately, in most practical applications, obtaining ultrasensitive plasmonic nanosensors is still a challenge. Dispersed analyte molecules are free to diffuse in throughout the volume of solution, which can be far from the plasmonic hot spot.[13,14] Considering the ultrasmall size of hot spots (sensitive down to few square nanometers), the probability of encountering analyte molecules in hot spots is very low. It has been demonstrated that the accumulation time is on the scale of days for detecting a few analyte molecules in a solution with at a femtomolar concentration.[15,16] For even dilute solutions, ultrasensitive detection is hardly achievable, partly because of the "diffusion limit" of analytes.

Developing strategies and techniques to overcome the "diffusion limit" is paramount for improving the sensitivity of plasmonic nanosensors, and this has drawn great research interest.[17-20] However, it is still a great challenge to develop a robust molecular enrichment strategy that can simultaneously concentrate a large volume solution and enrich analyte molecules into a small-sized sensitive area. For a highly dilute solution, very few analyte molecules are contained in a small volume of solution.[18,19] It is difficult to precisely locate so few molecules into a nanosized hot spot via analyte enrichment in a small volume of the solution.

Herein, inspired by the working principle of oil lamps, a robust molecular enrichment strategy is developed and investigated to concentrate a large volume of solution in a short time and effectively confines analyte molecules and Au NPs together into a small-sized sensitive region of plasmonic nanosensors. In this enrichment strategy, capillary force and heating evaporation are combined in a synergistic way to drive and enrich the few molecules present in highly dilute solutions into hot spots, enabling highly sensitive detection, even at femto- to attomolar (10^{-15}/10^{-18} mol L^{-1}) levels. The diffusion limit can be overcome, and time accumulation can be reduced to a few minutes. This robust but simple molecular enrichment strategy can be easily operated in various practical plasmonic-based sensing and detection.

EXPERIMENTAL SECTION

Materials: Chloroauric acid ($HAuCl_4 \cdot 4H_2O$), trisodium citrate ($Na_3C_6H_5O_7 \cdot 2H_2O$), crystal violet (CV) and anthracene were purchased from Sigma-Aldrich. Malachite green (MG) solution after purification process was obtained from Shaanxi Institute for Food and Drug Control. Mono-6-thio-β-cyclodextrin (HS-β-CD) was purchased from Tocopharm Corporation. Methamphetamine (METH) solution was obtained from Xi'an Jiaotong University Health Science Center. Glass microfiber filter (Whatman No.1820-047) was purchased from Whatman Corporation. All the chemical reagents were used without any further purification. Millipore Ultrapure water (18.2 MΩ) was used in all experiments.

Synthesis and modification of Au NPs: Citrate-stabilized Au NPs with average diameter of 50 nm was synthesized according to Frens' method.[34] Briefly, 100 mL of 0.25 mM $HAuCl_4$ solution was placed into a conical flask with oil bath. After the solution was boiled, 0.7 mL of 1 wt % sodium citrate solution was added immediately under magnetic stirring (500 rpm). The boiling mixture was continually heated for 45 min to give a brilliant red color, indicating the complete reduction of gold (III) ions. The obtained Au NPs were centrifuged and dispersed in alcohol solution to concentrate 50 times for further use. Furthermore, Au NPs were functionalized by mixing 1ml of Au NPs and 0.2 mL of 10^{-4} M HS-β-CD solution under stirring

overnight. The modified Au NPs were centrifuged and dispersed in alcohol solution for enrichment process.

Fabrication of enrichment device: A piece of GF paper was cut into rectangular geometry (5 mm X 18 mm). Top of the GF paper was clamped with a clip and flatly placed on heating plate. After the clip was heated by heating plate, the bottom of the GF paper was soaked in a mixture ethanol solution containing 1 mL of target analytes and 0.2 mL of concentrated Au NPs. The solution flowed up along the GF paper and volatilize at the edge of clip.

Purification process of MG in fish fillets: Briefly, 2.00 g of fish homogenates were mixed with 500 μL of 9.5 g/L hydroxylamine hydrochloride solution and dispersed by vortex. Then, the fish homogenates were mixed with acetonitrile (10 mL) and anhydrous magnesium sulfate (1.0 g). After vigorously vortexed for 1 min, Al_2O_3 (4.0 g) was added into the mixture to remove the lipids by vortex. The mixture was centrifuged and the supernatant was oxidized by adding 1 mL of 0.003 M oxidant 2,3-dichloro-5,6-dicyano-1,4-benzoquinone (DDQ) in acetonitrile and reaction for 10 min. Finally, the solution was filtered by the membrane prior for SERS detection.

Characterizations: The morphologies of Au NPs and GF paper were characterized by scanning electron microscope (SEM, JEOL, JSM-7000F). Raman spectra were collected using JY Horiba HR800 Raman system under the excitation of 633 nm laser. The laser beam was focused on the sample surface with a spot diameter of ~1 μm using a 50× objective. The exposure time was 30 s, and the laser power was 0.5 mW. Optical and fluorescence images were obtained with a Leica optical microscope (DM 4000M) using 10×objectives. At each concentration, 20 points are randomly selected and detected near position 1 or 7. All the SERS spectra were detected near the position 1 or 7(Figure 3a) if there is no special explanation in this article.

RESULTS AND DISCUSSION

Oil lamps (Figure 1a) are very ancient device that people invented for obtaining light or heat. The working principle of oil lamps is that the fuel, which is oil or an alcohol solution, is transported along a wick up to the head of the lamp where it is burned. Interestingly, the wick is a simple pump that can transport solution via the capillary force. On the basis of the working principle of alcohol lamps, we developed a molecular enrichment strategy for which the enrichment device is designed as shown in Figure 1b. A piece of glass fiber (GF) paper is used in the same manner as the wick of lamps. Specifically, the bottom part is soaked in a mixed solution that contains target analytes and Au NPs, and the top part is clamped with a clip. Similar with an alcohol lamp, the mixed solution is pumped from the bottom to the top, driven by the capillary force of the GF paper. By heating the clip, the solution is volatilized on the top of the GF paper. Thus, a continuous microflow of solution formed on the GF paper and transported analyte molecules and Au NPs to the edge of the clip. Volatilization of solvent is fastest at the surface of the GF paper that is nearest to the clip. There is a sharp gradient of solvent content on the GF paper along the edge from the clip to the outside. Thus, a great flowing force originated from the sharp gradient of solvent content and confined the analytes and Au NPs into a very small-sized region at the edge of the clip (Figure 1c). In this enrichment region, Au NPs are tightly aggregated together, and plenty of plasmonic hot spots form because of the gap enhancement effect between aggregated Au NPs. Analyte molecules are mixed with Au NPs and are well-located into hot spots. As a result, ultrasensitivity can be achieved for plasmonic-based molecule identification and detection in highly dilute solutions with techniques such as surface enhanced Raman spectroscopy (Figure 1d).

The working principle is derived from that of oil lamps, but the construction and function of our enrichment device are not exactly the same as oil lamps. To achieve robust and effective enrichment of analytes in a large volume of solution, several improvements were designed and implemented for the enrichment device. First, GF paper that consisted of micron-sized borosilicate GFs (Figure S1) was selected to transport the solution. The slippery surface of glass

microfibers promotes the microflow of solution and avoids blocking Au NPs during transport. In addition, the material, borosilicate GFs, has a heat-resistant temperature of 500 ℃, thus, the GF paper can not be deformed or damaged under the heating station in our experimental temperature (120 ℃). Second, the clip is used as a heating unit and also as a locking gate to stop the microflow of solution. On the other side, a linear heating region formed by clip on the GF paper that has stronger volatilizing ability for solvent than a spot area. Third, only one side of the clip is heated with a heating plate that can induce solvent volatilization and aggregation of Au NPs with analytes, and this is mainly on one side of the GF paper. Therefore, the enrichment ability increases. Figure S2 shows a TEM image and UV-vis spectrum of Au NPs that were synthesized and used in our enrichment study, which indicated that the particle size is uniform with a value of around 50 nm. As seen in Figure S3, after enrichment, Au NPs are tightly aggregated over a linear area with a width of around 100 μm.

The influences of operation conditions, such as heating temperature and length of GF paper, on the enrichment result were investigated, and the results are shown in Figure 2. Without Au NPs, when only analytes in ethanol solution (molecules of crystal violet (CV), 10^{-5} M, result in a violet color on GF paper) were used for enrichment, it is not relatively easy to confine only analyte molecules in a small-sized linear area (Figure 2a). With the conditions of a heating temperature of 120 ℃ and a length of GF paper of 8 mm or 13 mm, CV molecules can move through the edge of the clip and reach the area above the clip. Because the size of molecules is very small, the clip cannot thoroughly shut the channels of GF paper, and thus the movement of molecules through the clip is not prevented. When the length of the GF paper is increased to 18 mm, most of the CV molecules stay at the edge of the clip. This is because the ethanol solution is completely dried at the edge of the clip and CV molecules are transported through the clip without microflow. Thus, by optimizing the temperature and GF paper length, analyte molecules can be enriched into a relatively small-sized area. As seen in Figure 2a, 18 mm length of GF paper and a 120 ℃ heating temperature are the optimal conditions for enrichment. Most of the

CV molecules stay in the enrichment area on the heated side of the GF paper, and a small amount of CV molecules remain on the unheated side of the GF paper.

In contrast to the analyte molecules, Au NPs are relatively more easily confined into a small-sized area (Figure 2b). Au NPs are much larger than molecules that cannot move through the clip edge when the channels of GF paper are shut off by the clip. At a heating temperature of 120 ℃, Au NPs are well-confined into a small-sized area with different lengths of GF paper (8 mm, 13 mm, and 18 mm in Figure 2b). The same is true with CV molecules, as seen in Figure 2b; specifically, the optimal temperature for enrichment of Au NPs on 18 mm GF paper is 120 ℃. Figure 2c shows the enrichment results for different heating temperatures for the mixed ethanol solution containing CV molecules and Au NPs on 18 mm GF paper. When enriching with Au NPs, the CV molecules are well-confined into a small-sized area together with Au NPs. This is because aggregation of Au NPs blocks the tiny channels in GF paper at the edge of the clip and limits the movement of CV molecules through the clip. As seen in Figure 2c, the optimal temperature for enriching the mixed ethanol solution containing analyte molecules and Au NPs is also 120 ℃. As illustrated in Figure 2d, most of the analyte molecules and Au NPs were enriched on the heated side of the GF paper, and a small amount of them remained on the unheated side of the GF paper.

From the experimental results in Figure 2a-c, the detailed accumulation mechanism of AuNPs and CV molecules can be further deduced. As we previously presented and discussed in Figure 1, the capillary force and solvent evaporation function transferred AuNPs and CV to the heating area. With evaporation of solvent, AuNPs and CV were continuously accumulated at the heating region. On the other hand, the pressure of the tightly clamped clip on the GF paper also performed important function in the accumulation of AuNPs and CV. Under the pressure, the microchannels in the GF paper will be shut off, resulting in the blockage of AuNPs at the clip edge. The size of CV molecules is much smaller than AuNPs, thus part of CV would diffuse through the clip edge as only CV was used for the enrichment, and the accumulation area was

not small (Figure 2a). While, mixed with Au NPs, the aggregation of Au NPs would further block the CV at the clip edge. Thus, the accumulation area would become very small when mixture of Au NPs and CV was enriched. As shown in Figure S4, Au NPs were not blocked and aggregated at the clip edge when loose clip was used in the enrichment experiment.

Distributions of analyte molecules in the enriched area were investigated using SERS and fluorescence imaging. After enriching 1.2 mL of ethanol solution containing 0.2 mL of Au NPs and 1 mL of 10^{-5} M CV, seven points (marked as 1 to 7) along the lateral direction and three points (marked as I to III) along the vertical direction of the enriched area were selected for SERS characterization (Figure 3a). Figure 3b shows that the intensities of SERS signals for CV molecules at points 1 and 7 are stronger than those of SERS signals for CV at points 2 to 6. This phenomenon can be attributed to the lateral microflow of solution in GF paper.[17,21,22] The volatilization surface is larger at the two edges of the GF paper, and this results in faster volatilization of solution. More solution flowed to points 1 and 7, which were enriched; thus, stronger SERS signals were obtained. Similarly, volatilization closer to the heating clip is faster. Thus, more solution was enriched at the top of the enriched region, and stronger SERS signal was correspondingly obtained (Figure 3c). Figure S5 shows an optical image and the corresponding fluorescence image of the enriched area. Figures 3d and e are corresponding magnified images of the enriched area. As indicated by the dark area, Au NPs are confined to a linear area with a width of about 100 μm. Because of the quenching effect, the fluorescence of CV molecules disappeared in the region of Au NP aggregation. Even so, we found that the intensity of fluorescence decreased quickly along the distance to the upper edge of the Au NPs aggregates. Combined with the SERS results, we deduce that CV molecules were well-enriched and confined in a small-sized area that was centered at the upper edge of Au NP aggregates.

To further study the molecular enrichment ability of this strategy, we performed SERS measurements with enrichment volumes of CV solutions (10^{-9} M) ranging from 0.2 to 1.0 mL. Figure S6 shows that the Raman intensity of CV molecules increases in a nearly linear

relationship to the enrichment volume of the CV solution. The results indicate that no matter how many volumes of CV solution are enriched, the CV molecules are well-confined to the small-sized sensitive area with tightly aggregated Au NPs, and this induces a constant increase in the Raman intensity with an increase in the enrichment volume of CV solution. This current enrichment strategy possesses the ability to confine analyte into small-sized sensitive area and also has the capacity to enrich large volume solutions in a short amount of time. As seen in Figure S7, only 8 min are needed to enrich CV molecules in 1 mL of solution using a heating temperature of 120 ℃. Compared to the reported method of droplet enrichment on hydrophobic surfaces (usually an volume of 50 μL with an enrichment time of 6 min),[18] this method enriches a greater amount of solution in a short amount of time, which is a great advantage and indicates potential use in molecular enrichment. Figure S8 shows that the enrichment times have a nearly linear feature with each heating temperature and solution volume.

Changes in signal intensity (typical Raman peaks of CV molecules at 1171 cm^{-1} and 1612 cm^{-1} bands) versus CV concentration are plotted in Figure 4a and b. Also, as seen in Figure S9 and S10, the probability of obtaining observable SERS signals with different CV concentrations was also evaluated from the SERS spectra obtained at 20 different points that were randomly distributed near point 7 (marked in Figure 3a). We found that at high concentrations (10^{-9} to 10^{-12} M), the decrease in Raman intensity maintains a nearly linear relationship with a decrease in CV concentration, and there is a 100% probability that observable SERS signals are obtained (Figure 4c). Meanwhile, at relatively low CV concentrations (10^{-13} to 10^{-16} M), the decrease in Raman intensity is slow with respect to the decrease in CV concentration (Figure 4b), and the probability for observable SERS signals decreases dramatically (Figure 4c). This result may be explained using the schematic diagram provided in Figure S11. At high CV concentrations, the decrease of Raman intensity is induced by the decreased number of hot spots that adsorbed CV molecules (HSs-CV) in the detection area. At low CV concentrations, the density of HSs-CV becomes very low, such that the probability of HSs-CV being covered in the detection area

decreases. Thus, the Raman intensity does not decreased much if only the HSs-CV are covered in the detection area, but the probability for the observable SERS signals decreases quickly with a decrease in CV concentration. Figure 4d shows deviations of the Raman intensity at peaks of 1171 and 1612 cm^{-1} with a CV concentration of 10^{-9} M. The calculated deviations are 19.8% and 18.3% at peaks of 1171 and 1612 cm^{-1}, respectively, and this shows the uniformity of Raman intensity obtained with the enrichment strategy. At lower concentrations (10^{-12} M and blow), the fluctuation of SERS intensity became lager (Figure S10). Some detection points have CV Raman signals, while other points have no signals. When CV concentration decrease to very low level, the distribution of CV molecular would become very uneven on the SERS substrate. As shown in Figure S11, only when the CV molecule that located at hot spot was covered by the laser spot, the Raman signals could be detected. Otherwise, no Raman signals could be detected.

In the past, people found that some apolar or low-polar analyte molecules show reduced detection ability in SERS measurements.[24,26,27] This is partly because molecules, such as persistent organic pollutants (POPs), have weak interactions with Au NPs and thus are hardly attached to the hot spots. To further improve the sensitivity for detection of apolar or low-polar analyte using the enrichment strategy, we modified the Au NPs with mono-6-thio-β-cyclodextrin (HS-β-CD). HS-β-CD molecules have strong interactions with POP molecules.[24,26,27] As seen in Figure 5a, with the HS-β-CD modification, Au NPs have the ability to capture POP molecules into the hydrophobic cavity of HS-β-CD molecules. We used anthracene, which is a typical POPs, to evaluate the detection sensitivity of the enrichment strategy coupled with the modification of Au NPs. Raman spectra (Figure S12) indicate that Au NPs were successfully modified with HS-ß-CD. As seen in Figure 5b, the LOD of anthracene was improved to 10^{-10} M with the use of the modified Au NPs; this is two orders higher than the LOD obtained using bare Au NPs. Compared with nonenriched SERS detection for anthracene using HS-β-CD-modified Au nanostructures,[28-29] the LOD of our current strategy shows 2-3 orders of higher sensitivity.

The application of this current enrichment strategy was used in SERS detection of real samples. Malachite green (MG) is a harmful dye that has been extensively used in aquaculture for preventing and treating external fungal and parasitic infections in fish. The real samples extracted MG in fish fillets containing different MG concentrations were detected using the enrichment SERS technique. Figure 6a shows SERS spectra of the real samples with MG concentrations ranging from 100 ppb to 0.1 ppb. Characteristic Raman peaks at 796 and 1613 cm^{-1} are assigned to MG and were still be clearly identified at a concentration of 0.1 ppb. The LOD of real samples for MG was improved to two orders of magnitude lower than the minimum required performance limit of MG (2 ppb).[30]

Drug abuse is one of the world wide problems in the field of public safety. Particularly, methamphetamine (METH) is a typical representative of widely circulated drugs for low cost, ease of synthesis and strong addictive properties which can affect physical and mental capacities and may lead to death.[31] Here, we applied the enrichment SERS technique in the detection of the trace of METH. Figure 6b shows the obtained SERS spectra of METH with concentrations ranging from 1 ppm to 5 ppb. The corresponding SERS spectra presented clear fingerprint peaks of METH molecules at 1001 and 1029 cm^{-1}.[32] The detection limit could be as low as 5 ppb with high signal-to-noise. Compared with nonenriched SERS detection for METH, the LOD of enrichment SERS technique shows 2-3 orders of higher sensitivity. [33]

CONCLUSIONS

In summary, we developed a new molecular enrichment strategy that combines the capillary action of GF paper with the solvent evaporation effect. With a good design of the device and use of optimized the operation conditions, analyte molecules and Au NPs can be effectively confined to a small-sized area. At the same time, this strategy shows a robust enrichment ability, capable of condensing 1.0 mL of CV solution in 8 min. With the use of this enrichment strategy, the sensitivity of plasmonic nanosensors is significantly improved, and SERS detection for CV decreases to 10^{-16} M. To effectively confine apolar or low-polar analyte

molecules that have a weak affinity for Au NPs into hot spots, Au NPs were modified and used with this current enrichment method. By modifying of Au NPs with HS-β-CD, SERS detection sensitivity for a typical POP (anthracene) was decreased to 10^{-10} M. In the detection of real samples, the LOD of MG was two orders of magnitude lower than the minimum required performance limit. In brief, the current enrichment strategy is very robust, has easy operation, and effectively confines analyte into hot spots. We anticipate that the current enrichment strategy could meet emerging needs in ultrasensitive biological sensing, environmental pollution monitoring, food safety evaluation, and defense applications.

ASSOCIATED CONTENT

Supporting Information

Supporting Information Available: The following files are available free of charge.

SEM image of GF paper, Au NPs, and Au NPs and CV molecules enriched on the GF paper, optical and fluorescence image of the heating region, SERS spectra of CV molecules obtained by enriching different volumes of CV, schematic illustration of the changing of Raman intensity and probability for obtaining observable SERS signals, Raman spectra of HS-ß-CD powder and HS-ß-CD modified Au NPs.

AUTHOR INFORMATION

Corresponding Authors:

*E-mail: jxfang@mail.xjtu.edu.cn.

*E-mail: hjyou@mail.xjtu.edu.cn.

*E-mail: chenteng@xjtu.edu.cn

Notes

The authors declare no competing financial interest.

ACKNOWLEDGMENTS

This work was supported by the programs supported by the National Natural Science Foundation of China (No. 21675122, 21874104), the State's Key Project of Research and Development Plan (2017YFB0402800), Shaanxi Province Key Industries Innovation Chain Project (2019ZDLSF07-08), the World-Class Universities (Disciplines), the Characteristic Development Guidance Funds for the Central Universities, Basic Public Welfare Research Project of Zhejiang Province (No. LY20E010007) and Natural Science Foundation of Shaanxi Province (No. 2019JLP-19).

REFERENCES

(1) Garcia-Rico, E.; Alvarez-Puebla, R. A.; Guerrini, L. Direct surface-enhanced Raman scattering (SERS) spectroscopy of nucleic acids: from fundamental studies to real-life applications. *Chem. Soc. Rev.* **2018,** *47*, 4909-4923.

(2) Lee, H. K.; Lee, Y. H.; Koh, C. S. L.; Gia Chuong, P.-Q.; Han, X.; Lay, C. L.; Sim, H. Y. F.; Kao, Y.-C.; An, Q.; Ling, X. Y. Designing surface-enhanced Raman scattering (SERS) platforms beyond hotspot engineering: emerging opportunities in analyte manipulations and hybrid materials. *Chem. Soc. Rev.* **2019,** *48*, 731-756.

(3) Granger, J. H.; Schlotter, N. E.; Crawford, A. C.; Porter, M. D. Prospects for point-of-care pathogen diagnostics using surface-enhanced Raman scattering (SERS). *Chem. Soc. Rev.* **2016,** *45*, 3865-3882.

(4) Cialla-May, D.; Zheng, X. S.; Weber, K.; Popp, J. Recent progress in surface-enhanced Raman spectroscopy for biological and biomedical applications: from cells to clinics. *Chem. Soc. Rev.* **2017,** *46*, 3945-3961.

(5) Le Ru, E. C.; Meyer, M.; Blackie, E.; Etchegoin, P. G. Advanced aspects of electromagnetic SERS enhancement factors at a hot spot. *J. Raman Spectrosc.* **2008,** *39*, 1127-1134.

(6) Giannini, V.; Fernandez-Dominguez, A. I.; Heck, S. C.; Maier, S. A. Plasmonic Nanoantennas: Fundamentals and Their Use in Controlling the Radiative Properties of

Nanoemitters. *Chem. Rev.* **2011,** *111*, 3888-3912.

(7) Lim, D.-K.; Jeon, K.-S.; Hwang, J.-H.; Kim, H.; Kwon, S.; Suh, Y. D.; Nam, J.-M. Highly uniform and reproducible surface-enhanced Raman scattering from DNA-tailorable nanoparticles with 1-nm interior gap. *Nat. Nanotechnol.* **2011,** *6*, 452-460.

(8) Fang, J.; Du, S.; Lebedkin, S.; Li, Z.; Kruk, R.; Kappes, M.; Hahn, H. Gold Mesostructures with Tailored Surface Topography and Their Self-Assembly Arrays for Surface-Enhanced Raman Spectroscopy. *Nano Lett.* **2010,** *10*, 5006-5013.

(9) Ma, C.; Gao, Q.; Hong, W.; Fan, J.; Fang, J. Real-Time Probing Nanopore-in-Nanogap Plasmonic Coupling Effect on Silver Supercrystals with Surface-Enhanced Raman Spectroscopy. *Adv. Funct. Mater.* **2017,** *27* , 1603233.

(10) de Nijs, B.; Benz, F.; Barrow, S. J.; Sigle, D. O.; Chikkaraddy, R.; Palma, A.; Carnegie, C.; Kamp, M.; Sundararaman, R.; Narang, P.; Scherman, O. A.; Baumberg, J. J., Plasmonic tunnel junctions for single-molecule redox chemistry. *Nat. Commun.* **2017,** *8,* 994.

(11) Zhan, P.; Wen, T.; Wang, Z.-g.; He, Y.; Shi, J.; Wang, T.; Liu, X.; Lu, G.; Ding, B. DNA Origami Directed Assembly of Gold Bowtie Nanoantennas for Single-Molecule Surface-Enhanced Raman Scattering. *Angew. Chem. Int. Edit.* **2018,** *57*, 2846-2850.

(12) Chen, H.-Y.; Lin, M.-H.; Wang, C.-Y.; Chang, Y.-M.; Gwo, S. Large-Scale Hot Spot Engineering for Quantitative SERS at the Single-Molecule Scale. *J. Am. Chem. Soc.* **2015,** *137*, 13698-13705.

(13) Fang, Y.; Seong, N. H.; Dlott, D. D. Measurement of the distribution of site enhancements in surface-enhanced Raman scattering. *Science* **2008,** *321*, 388-392.

(14) Michaels, A. M.; Jiang, J.; Brus, L. Ag nanocrystal junctions as the site for surface-enhanced Raman scattering of single Rhodamine 6G molecules. *J. Phys. Chem. B* **2000,** *104*, 11965-11971.

(15) Nair, P. R.; Alam, M. A. Performance limits of nanobiosensors. *Appl. Phys. Lett.* **2006,** *88*, 233120.

(16) Sheehan, P. E.; Whitman, L. J. Detection limits for nanoscale biosensors. *Nano Lett.* **2005,** *5*, 803-807.

(17) Zhang, K.; Zhao, J.; Xu, H.; Li, Y.; Ji, J.; Liu, B. Multifunctional Paper Strip Based on Self-Assembled Interfacial Plasmonic Nanoparticle Arrays for Sensitive SERS Detection. *ACS Appl. Mater. Inter.* **2015,** *7*, 16767-16774.

(18) Yang, S.; Dai, X.; Stogin, B. B.; Wong, T.-S. Ultrasensitive surface-enhanced Raman scattering detection in common fluids. *P. Natl. Acad. Sci. USA.* **2016,** *113*, 268-273.

(19) De Angelis, F.; Gentile, F.; Mecarini, F.; Das, G.; Moretti, M.; Candeloro, P.; Coluccio, M. L.; Cojoc, G.; Accardo, A.; Liberale, C.; Zaccaria, R. P.; Perozziello, G.; Tirinato, L.; Toma, A.; Cuda, G.; Cingolani, R.; Di Fabrizio, E. Breaking the diffusion limit with super-hydrophobic delivery of molecules to plasmonic nanofocusing SERS structures. *Nat. Photonics* **2011,** *5*, 683-688.

(20) Zhang, D.; You, H.; Yuan, L.; Hao, R.; Li, T.; Fang, J. Hydrophobic Slippery Surface-Based Surface-Enhanced Raman Spectroscopy Platform for Ultrasensitive Detection in Food Safety Applications. *Anal. Chem.* **2019,** *91*, 4687-4695.

(21) Abbas, A.; Brimer, A.; Slocik, J. M.; Tian, L.; Naik, R. R.; Singamaneni, S. Multifunctional Analytical Platform on a Paper Strip: Separation, Preconcentration, and Subattomolar Detection. *Anal. Chem.* **2013,** *85*, 3977-3983.

(22) Yu, W. W.; White, I. M. Inkjet-printed paper-based SERS dipsticks and swabs for trace chemical detection. *Analyst* **2013,** *138*, 1020-1025.

(23) Bekana, D.; Liu, R.; Amde, M.; Liu, J.-F. Use of Polycrystalline Ice for Assembly of Large Area Au Nanoparticle Superstructures as SERS Substrates. *ACS Appl. Mater. Inter.* **2017,** *9*, 513-520.

24.Chen, B.; Meng, G.; Huang, Q.; Huang, Z.; Xu, Q.; Zhu, C.; Qian, Y.; Ding, Y. Green Synthesis of Large-Scale Highly Ordered Core@Shell Nanoporous Au@Ag Nanorod Arrays as Sensitive and Reproducible 3D SERS Substrates. *ACS Appl. Mater. Inter.* **2014,** *6*, 15667-15675.

(25) Ling, D.; Wu, Z.; Li, S.; Zhao, W.; Ma, C.; Wang, J.; Jiang, Z.; Zhong, Z.; Zheng, Y.; Yang, X. Large-Area Au-Nanoparticle-Functionalized Si Nanorod Arrays for Spatially Uniform Surface-Enhanced Raman Spectroscopy. *Acs Nano* **2017,** *11*, 1478-1487.

(26) Hou, C.; Meng, G.; Huang, Q.; Zhu, C.; Huang, Z.; Chen, B.; Sun, K. Ag-nanoparticle-decorated Au-fractal patterns on bowl-like-dimple arrays on Al foil as an effective SERS substrate for the rapid detection of PCBs. *Chem. Commun.* **2014,** *50*, 569-571.

(27) Zhu, C.; Meng, G.; Huang, Q.; Li, Z.; Huang, Z.; Wang, M.; Yuan, J. Large-scale well-separated Ag nanosheet-assembled micro-hemispheres modified with HS-beta-CD as effective SERS substrates for trace detection of PCBs. *J. Mater. Chem.* **2012,** *22*, 2271-2278.

(28) Xie, Y.; Wang, X.; Han, X.; Song, W.; Ruan, W.; Liu, J.; Zhao, B.; Ozaki, Y. Selective SERS detection of each polycyclic aromatic hydrocarbon (PAH) in a mixture of five kinds of PAHs. *J. Raman Spectrosc.* **2011,** *42*, 945-950.

(29) Gu, X.; Tian, S.; Zhou, Q.; Adkins, J.; Gu, Z.; Li, X.; Zheng, J. SERS detection of polycyclic aromatic hydrocarbons on a bowl-shaped silver cavity substrate. *RSC Adv.* **2013,** *3*, 25989-25996.

(30) Guo, Z.; Gai, P.; Hao, T.; Duan, J.; Wang, S. Determination of Malachite Green Residues in Fish Using a Highly Sensitive Electrochemiluminescence Method Combined with Molecularly Imprinted Solid Phase Extraction. *J. Agr. Food Chem.* **2011,** *59*, 5257-5262.

(31) Stojanovska, N.; Fu, S.; Tahtouh, M.; Kelly, T.; Beavis, A.; Kirkbride, K. P. A review of impurity profiling and synthetic route of manufacture of methylamphetamine, 3,4-methylenedioxymethylamphetamine, amphetamine, dimethylamphetamine and p-methoxyamphetamine. *Forensic Sci. Int.* **2013,** *224*, 8-26.

(32) Dong, R.; Weng, S.; Yang, L.; Liu, J. Detection and Direct Readout of Drugs in Human Urine Using Dynamic Surface-Enhanced Raman Spectroscopy and Support Vector Machines. *Anal. Chem.* **2015,** *87*, 2937-2944.

(33) Weng, S.; Dong, R.; Zhu, Z.; Zhang, D.; Zhao, J.; Huang, L.; Liang, D. Dynamic surface-

enhanced Raman spectroscopy and Chemometric methods for fast detection and intelligent identification of methamphetamine and 3,4-Methylenedioxy methamphetamine in human urine. *Spectrochim. Acta. A* **2018,** *189*, 1-7.

(34) Frens, G. Controlled nucleation for the regulation of the particle size in monodisperse gold suspensions. *Nat. Phys. Sci.* **1973,** *241*, 20-22.

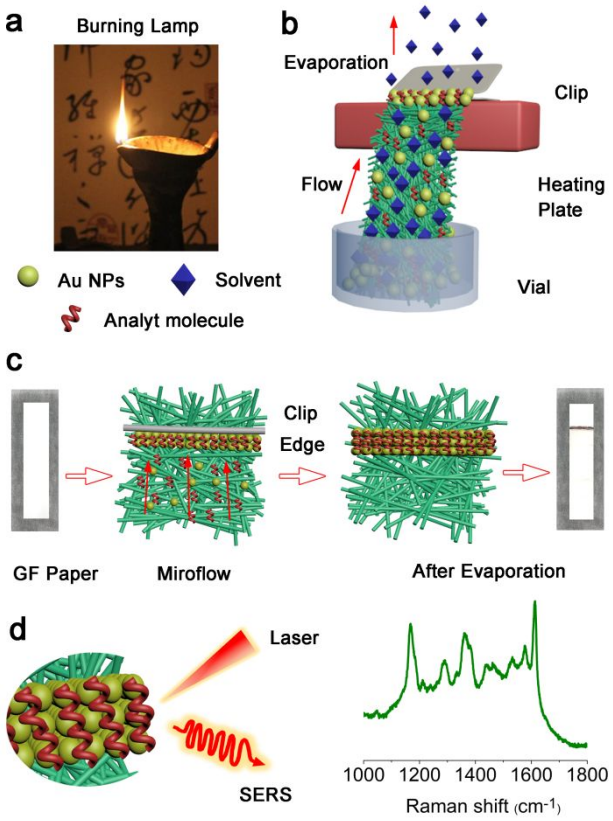

Figure 1. Schematic illustration of the working principle of enrichment device. (a) Image of an ancient oil lamp. (b) Construction of the molecular enrichment device. (c) The enrichment process that the solution transports analytes and Au NPs along the GF paper to the edge of the heating clip. (d) After the analytes and Au NPs are enriched together, SERS is greatly enhanced.

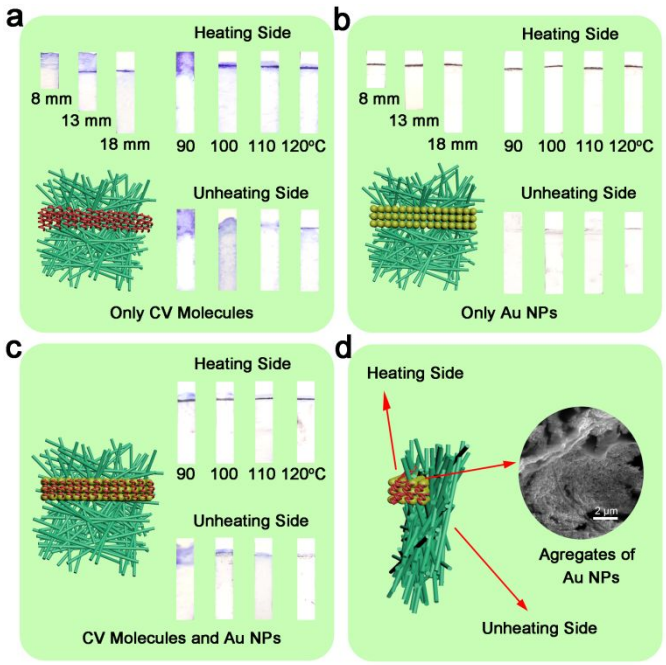

Figure 2. Enrichment result with different conditions. (a) Just CV molecules, (b) just Au NPs and (c) a mixture of CV molecules and Au NPs are enriched with different heating temperatures on GF papers of different lengths. (d) Schematic illustration and TEM image of CV molecules and Au NPs being transported and enriched at a high temperature side of the GF papers.

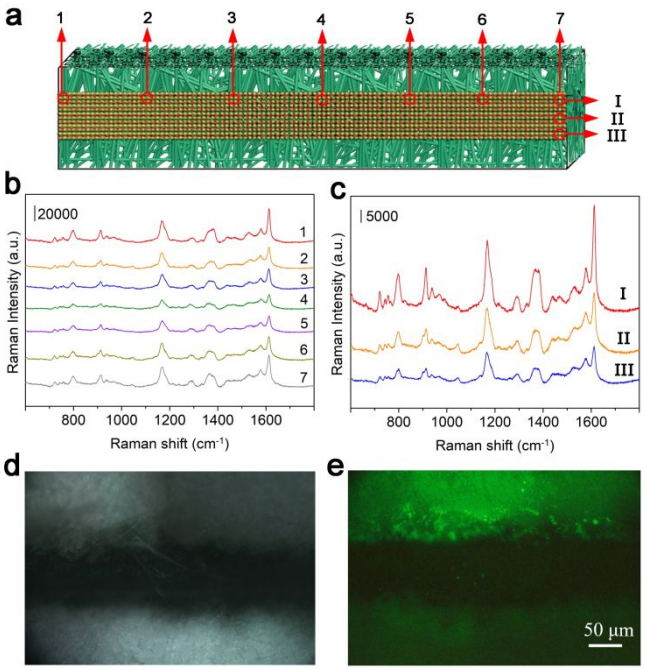

Figure 3. Distribution of CV molecules in the heated region. (a) Schematic illustrations of selected points for SERS measurement in the heated region. SERS spectra of CV molecules obtained at (b) points 1 to 7 and (c) points I to III. (d) Optical image and (e) correlated fluorescence image of the heated region.

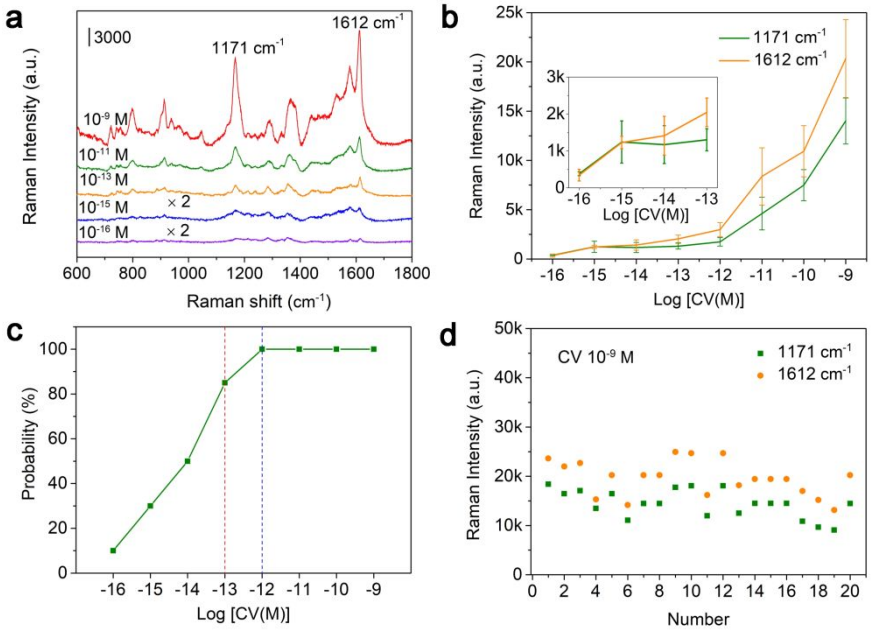

Figure 4. Plasmonic sensing properties based on molecular enrichment. (a) SERS spectra of CV molecules obtained from the enriched aqueous solution with different CV concentrations from 10^{-9} M to 10^{-16} M. (b) SERS intensity plot at peaks of 1171 and 1612 cm^{-1} versus CV concentration. (c) Probability of obtaining observable SERS signals with different CV concentrations. (d) Raman intensity deviations at peaks of 1171 and 1612 cm^{-1} with a CV concentration of 10^{-9} M.

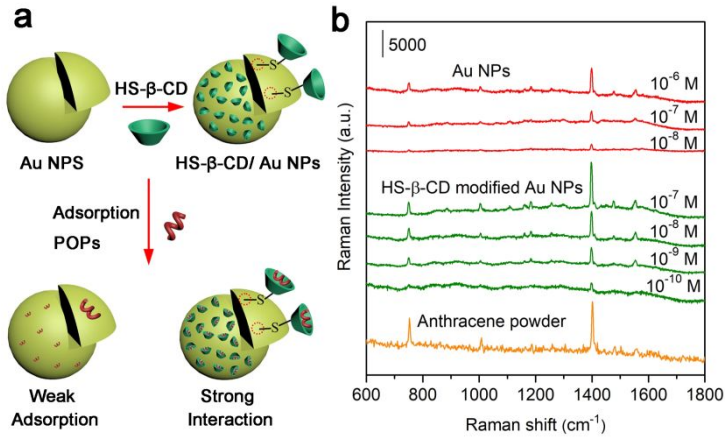

Figure 5. Plasmonic sensing properties based on molecular enrichment for POPs measurements. (a) Schematic illustrations of POPs affinity to bare Au NPs and to HS-ß-CD-modified Au NPs. (b) SERS spectra of anthracene (a typical POP) using bare Au NPs and HS-ß-CD-modified Au NPs with the enrichment strategy.

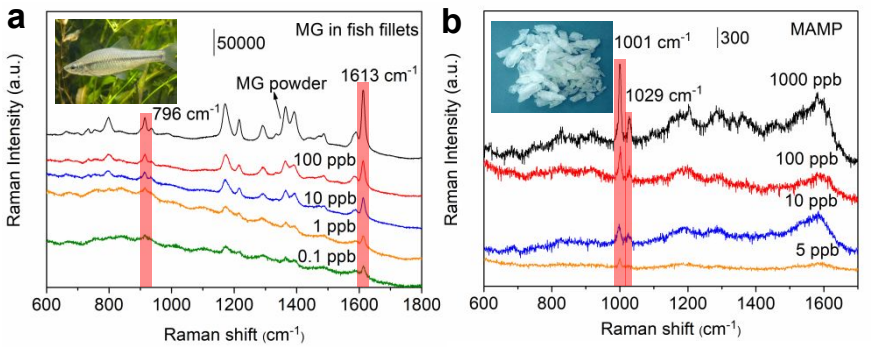

Figure 6. Plasmonic sensing properties based on molecular enrichment for malachite green (MG) in fish fillets and methamphetamine (METH). (a) SERS spectra of MG extracted from fish fillets with different concentrations. The detection solution of MG in fish fillets was extracted and treated by alumina to remove lipids and other components before the measurement. (b) SERS spectra of METH at different concentrations.

For TOC only